

In-Flight Estimation of Helicopter Gross Weight and Mass Center Location

Michael Abraham* and Mark Costello†

Georgia Institute of Technology, Atlanta, Georgia 30332

DOI: 10.2514/1.41018

The ability to compute the weight and balance of a helicopter in flight under general conditions is an enabling technology for future condition based maintenance systems as well as advanced automatic flight control systems. This paper creates a real-time weight and balance estimation algorithm using an extended Kalman filter framework. To highlight estimation characteristics, the algorithm is exercised on the OH-6A helicopter in a variety of flight regimes. The algorithm is examined in hover and forward flight as well as situations where loads are dropped and picked up in flight. For sample scenarios considered, the algorithm quickly estimates station line and butt line mass center position (1 s) and more slowly converges on helicopter weight (10 s). To estimate the helicopter waterline, the algorithm requires modest flight maneuvering where a nonzero roll rate is present. The algorithm is also shown to be reasonably robust relative to sensor and model errors with increasing estimation error with increasing levels of model mismatch and sensor error.

Nomenclature

I_B	=	flapping inertia of rotor blade
I_H	=	inertia matrix of helicopter about its mass center
L, M, N	=	Total moment on the helicopter about the mass center in the helicopter reference frame
m, W	=	mass and weight of helicopter
p, q, r	=	components of angular velocity of helicopter in the helicopter reference frame
R	=	rotor radius
T_H	=	transformation matrix from inertial reference frame to helicopter reference frame
u, v, w	=	components of mass center velocity of helicopter in the helicopter reference frame
X, Y, Z	=	total force on the helicopter in the helicopter reference frame
x, y, z	=	components of helicopter mass center position vector in an inertial frame
$\beta, \beta_0, \beta_{1C}, \beta_{1S}$	=	flapping angle, collective, longitudinal, lateral flapping angles
ϕ, θ, ψ	=	Euler roll, pitch, and yaw angles of helicopter

I. Introduction

IT IS well-known that weight and mass center location greatly affect static and dynamic characteristics of helicopters. These quantities are often manipulated during the design process to obtain desired performance from the aircraft. Safe operation of helicopters is a function of the weight of the aircraft and the location of the mass center. Sufficiently accurate in-flight estimation of the gross weight and mass center location can substantially improve overall performance of the air vehicle as these feedback signals can be put to good use within a condition based maintenance system, a health and usage monitoring system, the automatic flight control system, and mission planning software systems. Determining the useful life of

parts on helicopters relies on knowledge of how long the aircraft is in a given flight condition so that damage on components can be properly tallied. Since damage on components is a strong function of gross weight and mass center location, accurate and relatively frequent in-flight estimation of gross weight and mass center location help markedly enhance safety, reduce the operating cost of helicopters by removing parts on the aircraft at the end of their useful life, and avoid replacing parts too early or leaving them on the aircraft too long. Real-time weight and balance information can also be used for flight control. This is particularly true for heavy lift helicopters where it may be necessary to schedule gains in the flight control system as a function of the gross weight and mass center location to ensure adequate handling qualities over the operational envelope of the aircraft. Gain scheduling is often necessary to ensure integrity of the airframe by altering control inputs so as to limit flight loads on the structure.

While simple and straightforward, practical experience has shown that it is not feasible to rely on aircrew estimates of aircraft gross weight and center of gravity for most applications. The capability of helicopters to change gross weight, center of gravity position, and rotor thrust level during flight, or while the landing gear are in full or partial ground contact, makes reliable sensing of aircraft gross weight using strain gages installed on the landing gear an impractical means of estimating gross weight and center of gravity for most rotorcraft. More sophisticated methods have been developed, but all suffer from considerable limitations that preclude general use. Moffatt [1] created a simple algorithm to predict the weight of a helicopter which requires only engine torque, hover height, pressure altitude, and ambient temperature. The algorithm is based on the UH-1H hover performance chart found in the operator user manual. Morales and Haas [2] created a neural network algorithm to estimate the weight of a helicopter in hover. Although this work only addressed the hover flight regime, it showed the ability of neural networks to be properly trained on noisy flight test data, and subsequently employed for in-flight gross weight estimation. Idan et al. [3] also created a neural network based method to estimate gross weight along with the mass center of an aircraft in flight. To speed the training process for the neural network, basic flight mechanic relations were incorporated into the algorithm. Teal et al. [4] created a regime recognition algorithm for the MH-47E successful effort which estimated helicopter gross weight and the weight of externally slung cargo for all flight conditions using inertial sensor data and air data system measurements. The gross weight estimator is used in the MH-47E structural usage monitoring system (SUMS) to monitor fatigue life expenditure in life limited dynamic components. The gross weight estimation process described by Teal et al. uses

Received 15 September 2008; revision received 5 February 2009; accepted for publication 14 February 2009. Copyright © 2009 by the American Institute of Aeronautics and Astronautics, Inc. All rights reserved. Copies of this paper may be made for personal or internal use, on condition that the copier pay the \$10.00 per-copy fee to the Copyright Clearance Center, Inc., 222 Rosewood Drive, Danvers, MA 01923; include the code 0021-8669/09 \$10.00 in correspondence with the CCC.

*Graduate Research Assistant, School of Aerospace Engineering, Member AIAA.

†Sikorsky Associate Professor, School of Aerospace Engineering, Associate Fellow AIAA.

corrected moment theory to estimate shaft horsepower, and then uses the difference between the actual and estimated shaft horsepower to adjust the estimate of gross weight until the estimated power level tracks the actual power level. This algorithm estimates gross weight only and is not intended for real-time use.

This work presents a new approach to real-time in-flight estimation of helicopter gross weight and mass center location. An extended Kalman filter is constructed with a state vector consisting of weight and balance states as well as rigid vehicle states. A unique feature of the algorithm, as compared with existing methods, is its general applicability, including scenarios where the weight and balance changes due to dropping off and picking up loads. The developed algorithm is exercised on the OH-6A helicopter and results are presented as a function of different maneuvers and different levels of model and sensor error. This paper presents a fundamentally new technique to an important problem by combining a well established state estimation technique from control theory and accepted methods for flight dynamic modeling of rotorcraft. The work presented here also includes an initial exploration of the estimation algorithm's performance characteristics. The future of this technique is promising as the method is shown to work well in practical helicopter flight scenarios.

II. Helicopter Dynamic Model

For the work reported below, helicopter motion is simulated by modeling the aircraft as a rigid body with 6 degrees of freedom. This dynamic model provides a reasonable level of fidelity for the purposes of this investigation. This model is similar to a well-known helicopter dynamic model of comparable complexity such as ARMCOP [5] and is a compromise between more complex helicopter models such as FLIGHTLAB [6] and far simpler ones such as TMAN [7]. While flight dynamic models can be tuned to reproduce the behavior observed in flight tests, they are by no means perfect. There will always be a mismatch between motion predicted using a dynamic model and flight measurements.

The state vector consists of 12 state variables that describe position and velocity of the vehicle's mass center and the attitude and angular rates of the vehicle with respect to inertial space:

$$\begin{Bmatrix} \dot{x} \\ \dot{y} \\ \dot{z} \end{Bmatrix} = [T_H] \begin{Bmatrix} u \\ v \\ w \end{Bmatrix} \quad (1)$$

$$\begin{Bmatrix} \dot{\phi} \\ \dot{\theta} \\ \dot{\psi} \end{Bmatrix} = \begin{bmatrix} 1 & s_\phi t_\theta & c_\phi t_\theta \\ 0 & c_\phi & -s_\phi \\ 0 & s_\phi/c_\theta & c_\phi/c_\theta \end{bmatrix} \begin{Bmatrix} p \\ q \\ r \end{Bmatrix} \quad (2)$$

$$\begin{Bmatrix} \dot{u} \\ \dot{v} \\ \dot{w} \end{Bmatrix} = \begin{Bmatrix} X/m \\ Y/m \\ Z/m \end{Bmatrix} + \begin{bmatrix} 0 & -r & q \\ r & 0 & -p \\ -q & p & 0 \end{bmatrix} \begin{Bmatrix} u \\ v \\ w \end{Bmatrix} \quad (3)$$

$$\begin{Bmatrix} \dot{p} \\ \dot{q} \\ \dot{r} \end{Bmatrix} = [I_H]^{-1} \left[\begin{Bmatrix} L \\ M \\ N \end{Bmatrix} - [S_H][I_H] \begin{Bmatrix} p \\ q \\ r \end{Bmatrix} \right] \quad (4)$$

where

$$T_H = \begin{bmatrix} c_\theta c_\psi & c_\theta s_\psi & -s_\theta \\ s_\phi s_\theta c_\psi - c_\phi s_\psi & s_\phi s_\theta s_\psi + c_\phi c_\psi & s_\phi c_\theta \\ c_\phi s_\theta c_\psi + s_\phi s_\psi & c_\phi s_\theta s_\psi - s_\phi c_\psi & c_\phi c_\theta \end{bmatrix}$$

$$S_H = \begin{bmatrix} 0 & -r & q \\ r & 0 & -p \\ -q & p & 0 \end{bmatrix}$$

In the previous equations the normal shorthand notation for sine and cosine is employed: $s_\alpha = \sin(\alpha)$, $c_\alpha = \cos(\alpha)$.

The total forces and moments in the helicopter reference frame that appear in Eqs. (3) and (4) have contributions from helicopter weight, the main rotor, the tail rotor, fuselage aerodynamics, and empennage aerodynamics. Forces from each component are first found in that component's reference frame and then are transformed into the vehicle's body frame. Moment contributions from each component come from two sources: pure moments and moments due to the offset of the component's forces from the vehicle's center of mass.

The rotor model that is used for both the main rotor and tail rotor is a quasi-static combined blade-element/momentum-theory approach [8]. The model assumes rigid blades but accounts for twist, taper, and nonzero flapping hinge offset. First, harmonic flapping and uniform inflow is assumed,

$$\beta = \beta_0 + \beta_{1C} \cos(\psi_{MR}) + \beta_{1S} \sin(\psi_{MR}) \quad (5)$$

The differential equation that governs rotor flapping dynamics is given in the next equation:

$$\ddot{\beta} + \omega_N^2 \beta = M_F \quad (6)$$

where

$$\omega_N = \Omega \sqrt{\frac{I_B + \frac{m_e R}{2}}{I_B}} \quad (7)$$

$$M_F = -\frac{M_A}{I} - \frac{mgR}{2I} \quad (8)$$

At a given instant in time the quasi-steady rotor flapping angles, and subsequently the rotor loads, are computed by a harmonic balance procedure. Nonlinear algebraic collective, longitudinal, and lateral rotor flapping equations are formed as shown in the following equations:

$$\int_0^{2\pi} (\ddot{\beta} + \omega_N^2 \beta - M_F) d\psi_{MR} = 0 \quad (9)$$

$$\int_0^{2\pi} (\ddot{\beta} + \omega_N^2 \beta - M_F) c_{\psi_{MR}} d\psi_{MR} = 0 \quad (10)$$

$$\int_0^{2\pi} (\ddot{\beta} + \omega_N^2 \beta - M_F) s_\psi d\psi_{MR} = 0 \quad (11)$$

These equations are satisfied through selection of the rotor flapping angles β_0 , β_{1C} , and β_{1S} , and are numerically solved by a Newton-Raphson iteration scheme. It is important to note that pilot controls enter the rotor flapping equations through the right hand side forcing function. Force and moment contributions from the fuselage and empennage are modeled with aerodynamic table lookups.

An additional consideration when implementing this flight dynamic model alongside an algorithm for weight and balance parameter estimation is the vehicle moments of inertia. In the work presented here, the vehicle moments of inertia are adjusted from their nominal values as the estimates of mass center location and gross weight change.

III. Estimation Algorithm

The estimation algorithm seeks to compute the mass of the helicopter along with the three components of the mass center locations using rigid body aircraft motion feedback and an internal model of the helicopter (Fig. 1).

An extended Kalman filter is created with rigid aircraft position (x, y, z), orientation (ϕ, θ, ψ), translational velocity (u, v, w), angular velocity (p, q, r), aircraft mass (m), and aircraft mass center

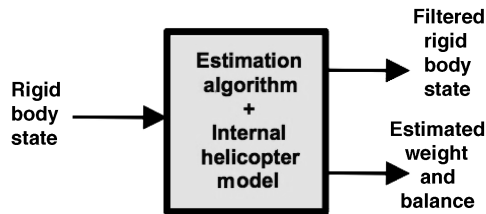


Fig. 1 Estimation algorithm schematic.

location (scg, bcg, wcg) as states. The extended Kalman filter is a trusted industry standard for state estimation processes. The nonlinear helicopter model described above is used for the internal aircraft model. The weight and balance of the helicopter is assumed to vary in a relatively slow manner and the dynamics of the weight and balance states are trivially assumed to be given in the following equations:

$$\dot{m} = 0 \quad (12)$$

$$\dot{x}_{CG} = 0 \quad (13)$$

$$\dot{y}_{CG} = 0 \quad (14)$$

$$\dot{z}_{CG} = 0 \quad (15)$$

The meta model of helicopter rigid body motion and weight and balance estimation states is cast together as a nonlinear dynamic system:

$$\dot{\zeta} = f(\zeta, \delta) + \varepsilon(t) \quad (16)$$

The vector δ contains control inputs consisting of collective, longitudinal cyclic, lateral cyclic and pedal. The vector ε is process noise. The meta state is split into the helicopter rigid body state and the mass and balance state:

$$\zeta_H = \begin{Bmatrix} x \\ y \\ z \\ \phi \\ \theta \\ \psi \\ u \\ v \\ w \\ p \\ q \\ r \end{Bmatrix} \quad \zeta_E = \begin{Bmatrix} m \\ x_{CG} \\ y_{CG} \\ z_{CG} \end{Bmatrix} \quad (17)$$

Measurements of the rigid body motion of the helicopter used as input to the estimation algorithm contain rigid body motion and noise:

$$\eta = h(\zeta, \delta) + \kappa(t) \quad (18)$$

In the previous equation, $\kappa(t)$ represents a vector of measurement noise.

Given the nonlinear system model above, an extended Kalman filter has five main steps associated with each estimation cycle: meta state propagation, meta state error covariance propagation, Kalman gain calculation, meta state Kalman filter update, and meta state error covariance Kalman filter update. This is depicted in Fig. 2.

Several of the steps in the Kalman filter require a linear state space dynamic model and a linear measurement model:

$$\dot{\zeta}(t) = A\zeta(t) + B\delta(t) \quad (19)$$

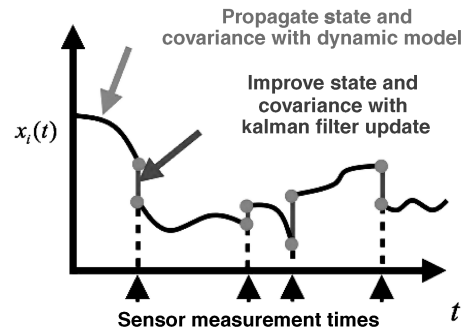


Fig. 2 Kalman filter schematic.

$$\eta(t) = C\zeta(t) \quad (20)$$

Of course, the state dynamic equations are highly nonlinear and a numerical, finite difference approach is used to obtain the needed derivatives for the linear time invariant dynamic model:

$$A = \frac{\partial f}{\partial \zeta}, \quad B = \frac{\partial f}{\partial \delta}, \quad C = \frac{\partial h}{\partial \zeta} \quad (21)$$

The meta state of the system is propagated forward in time by numerically integrating the equations of motion (Eq. (16)) with the process noise set to zero. The error covariance differential equation (Eq. (22)) is also numerically integrated in time to propagate itself forward:

$$\dot{P} = AP = PA^T + Q - PH^T R^{-1} HP \quad (22)$$

For the purposes of this paper, it is assumed that the vehicle's onboard sensors and associated signal processing packages have been given sufficient time to construct a useful rigid body state vector at the time the estimation algorithm is initiated. Because the initial rigid body state is assumed known, the associated elements of the P matrix are initially zero in this investigation. In Eq. (22), Q and R are the covariance matrices for the process noise and measurement noise, respectively. The performance of this filtering technique depends largely upon the selected values for Q and R . Because the parameter estimation process is cast in the guise of a state estimation process, the Q matrix is weighted heavily toward the unknown parameter states.

Aside from the linearization process of the helicopter plant, the most computationally expensive part of this estimation technique is calculating the Kalman gain matrix. The formula for the Kalman gain is provided in Eq. (23):

$$K = PH^T [HPH^T + R]^{-1} \quad (23)$$

Note that full state feedback is assumed and a 12×12 matrix must be inverted at each computation cycle. Because not all rigid body states contribute to the weight and mass center estimation (horizontal coordinates and heading angle), omitting the unneeded states from this algorithm would help to reduce computational requirements in practical implementation. For the sake of brevity, further discussion of the extended Kalman filter is omitted. More details on the extended Kalman filter can be found in [9,10].

IV. Results

To explore the viability of the above estimation scheme for real-time, in-flight helicopter gross weight and mass center location prediction, a set of simulation results have been generated for the OH-6A helicopter shown in Fig. 3 [11]. The OH-6A is a single-engine light helicopter with a four-blade main rotor used for personnel transport, escort and attack missions, and observation. The main rotor has a nondimensional twist of -0.14 , a flapping hinge offset of 0.46 ft, a radius of 13.17 ft, a rotational speed of 50.58 rad/s, a blade mass of 1.16 slugs, a flapping inertia of 46.83 slug ft², and an average chord of 0.56 ft. The main rotor is



Fig. 3 OH-6A helicopter.

located at station line 100.0 in., butt line 0.0 in., and waterline of 100.0 in.

The tail rotor is a two blade system with a nondimensional twist of -0.14 , a radius of 1.13 ft, and a rotational speed of 326.1 rad/s. The tail rotor is located at station line 282.00 in., butt line -11.6 in., and water line 71.3 in. The nominal gross weight of the vehicle is 2550 lbf. The nominal mass center location is station line 100.0 in., butt line 0.0 in., and water line 49.6 in.

Figures 4–7 show relevant aircraft motion for a maneuver used to test the algorithm. In the maneuver, the OH-6A is in forward flight at a reasonably steady speed and at nearly constant pitch attitude. The aircraft is maneuvering in the lateral channel with roll angle excursions on the order of 50 deg over a 20 s period, ranging from +20 deg to -30 deg (Fig. 4) with associated peak roll rates of 30 deg/s (Fig. 6). The aircraft also has heading oscillations from +20 deg to -40 deg (Fig. 5) with peak yaw rates of 7 deg/s. During this maneuver condition, the aircraft maintains constant

altitude and swerves modestly. Control activity is modest with main rotor collective settling around 12.5 deg and cyclic pitch oscillations of under 2 deg in both channels. For this maneuver, weight and balance estimation results are shown in Figs. 8–11. The estimator is turned on at $t = 0$ s with the initial gross weight in error by 250 lbf and the initial mass center station line, butt line, and water line in error by 2, 2, and 1 in., respectively. The Kalman filter weighting matrices are set to 0.02 for the rotorcraft states, 1000 for the weight and balance states with the exception of the water line state which is set to 2000, and 1.0 for the measurement noise. The weight and mass center water line are effectively estimated in slightly less than 10 s (Figs. 8 and 11). Converged estimates for the mass center station line and butt line occur much more rapidly (Figs. 9 and 10). Estimation of

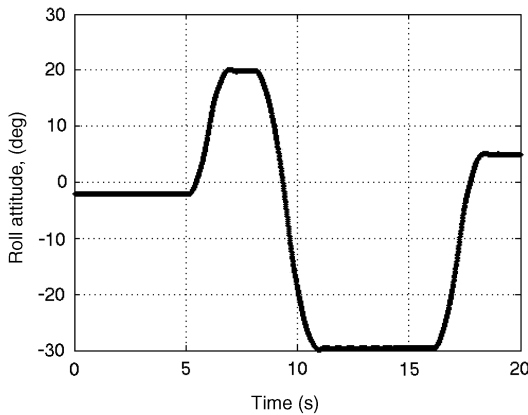


Fig. 4 Roll angle.

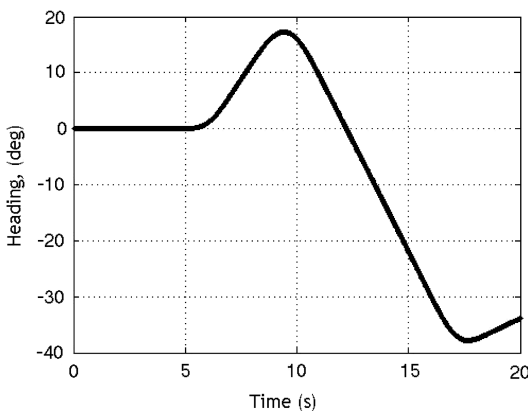


Fig. 5 Yaw angle.

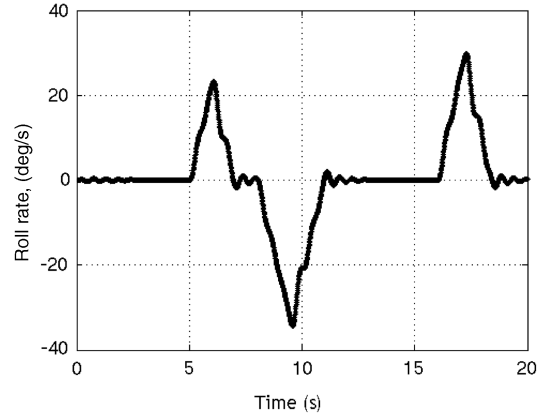


Fig. 6 Roll rate.

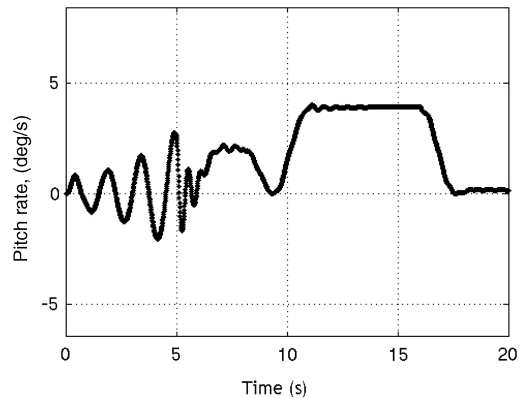


Fig. 7 Pitch rate.

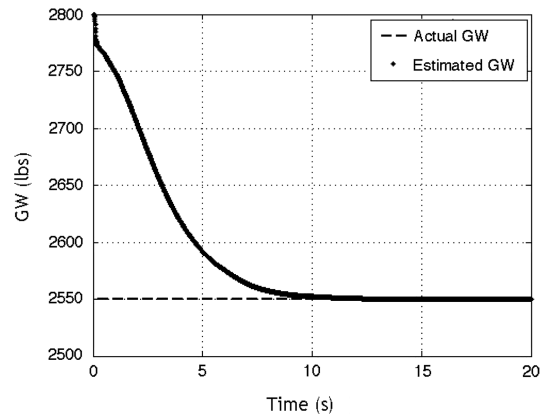


Fig. 8 Gross weight estimation in forward flight; (GW denotes gross weight).

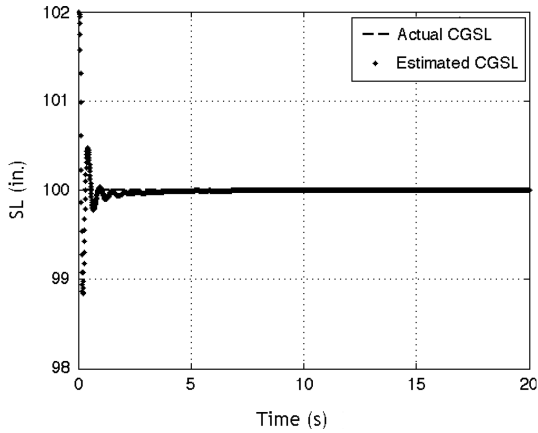


Fig. 9 Mass center station line estimation in forward flight; (SL denotes station line; CGSL denotes center of gravity station line).

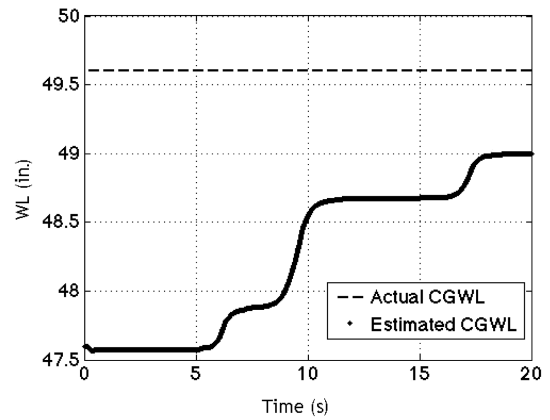


Fig. 12 Mass center water line estimation in forward flight (poor initial guess); (WL denotes water line).

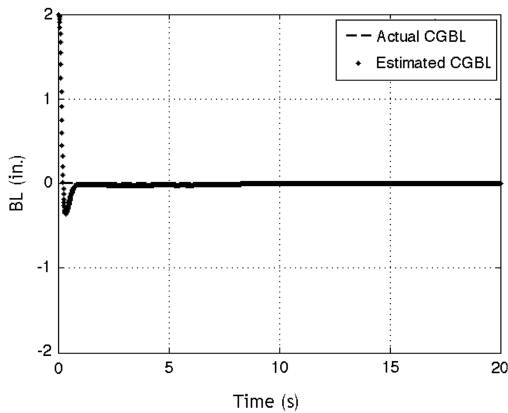


Fig. 10 Mass center butt line estimation in forward flight; (BL denotes butt line; CGBL denotes center of gravity butt line).

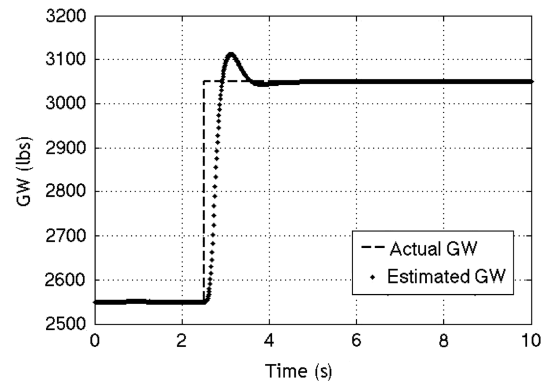


Fig. 13 Gross weight estimation in hover; (GW denotes gross weight).

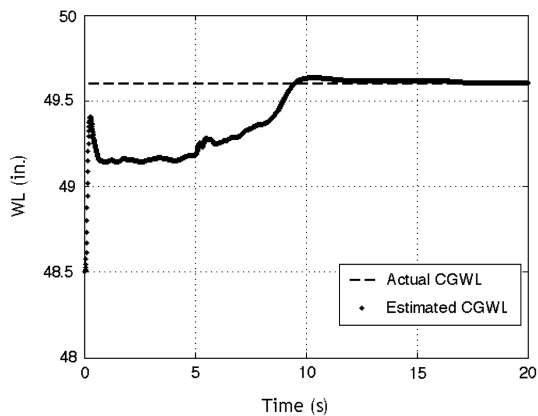


Fig. 11 Mass center water line estimation in forward flight; (WL denotes water line; CGWL denotes center of gravity water line).

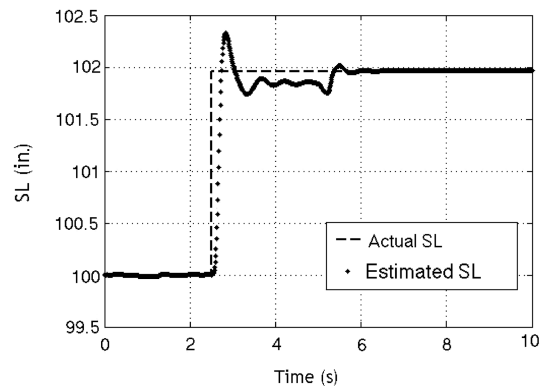


Fig. 14 Mass center station line estimation in hover; (SL denotes station line).

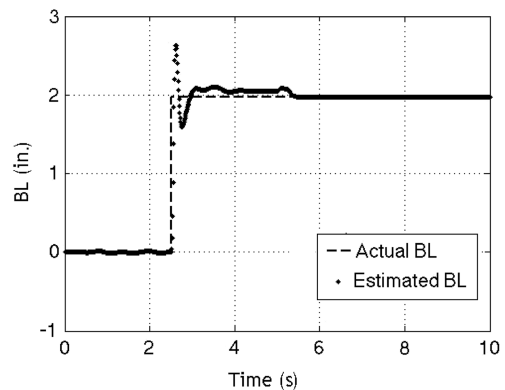


Fig. 15 Mass center butt line estimation in hover; (BL denotes butt line).

the mass center water line is tricky and requires aircraft roll rate to render the water line observable with the estimation filter. The filter data shown in Fig. 12 is a result of a poorly weighted Q matrix and a large initial error in waterline estimation (2 in.). By viewing the aircraft roll rate (Fig. 6) alongside Fig. 12 it is clear that estimation of the water line requires the roll rate to progress toward the actual value. The results shown are typical for forward flight.

Figures 13–16 present estimation results for a hover case in which the weight and mass center location are suddenly changed due to a 500 lbf load added below and to the right of the original mass center location. For the first 2.5 s of the hover, the vehicle is at baseline

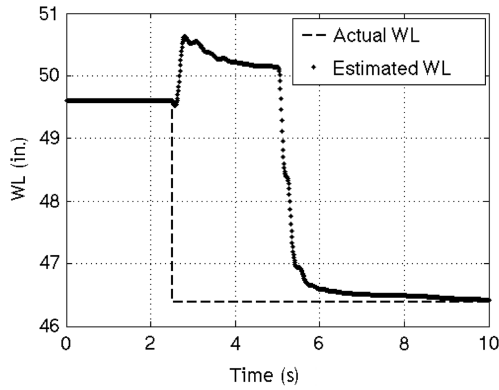


Fig. 16 Mass center water line estimation in hover; (WL denotes water line).

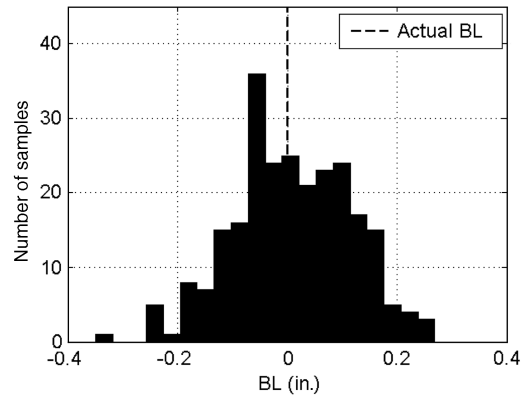


Fig. 19 Histogram of mass center butt line estimation with sensor noise; (BL denotes butt line).

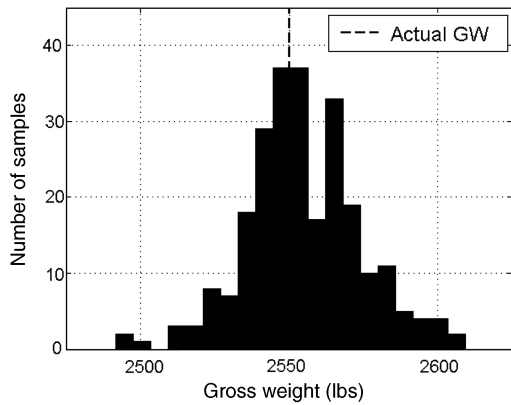


Fig. 17 Histogram of gross weight estimation with sensor noise; (GW denotes gross weight).

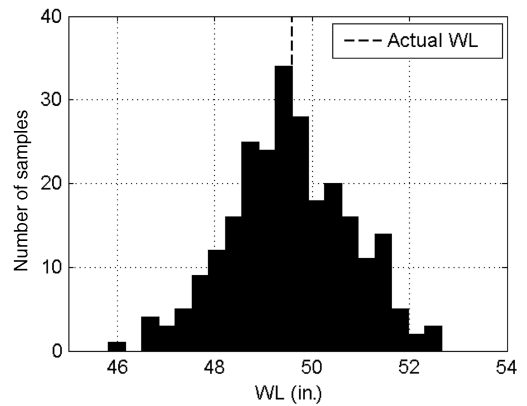


Fig. 20 Histogram of mass center water line estimation with sensor noise; (WL denotes water line).

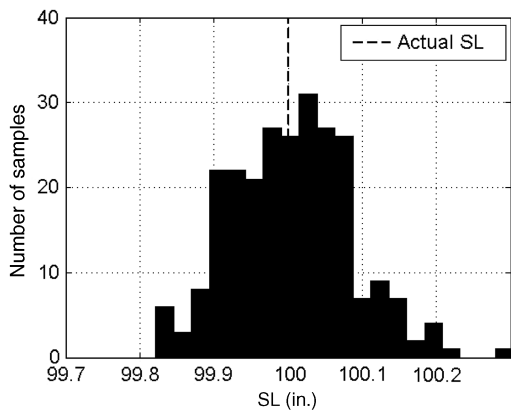


Fig. 18 Histogram of mass center station line estimation with sensor noise; (SL denotes station line).

values of weight = 2550 lbf, mass center station line = 100 in., mass center butt line = 0.0 in., and mass center water line = 49.6 in.. After the weight is added, weight = 3050 lbf, mass center station line = 102 in., mass center butt line = 2.0 in., and mass center water line = 46.4 in.. When the weight is added, the estimation algorithm is reinitiated so that the filter can immediately adjust to changes in weight and balance properties. Because Eqs. (12–15) constrain the weight and balance parameters to be constant, this resetting is necessary if any sudden changes in gross weight or mass center location occur. At $t = 5$ s, the vehicle begins a benign maneuver in which it picks up a small amount of flight speed and banks a small amount. The Kalman filter weighting matrices are set the same as in the previous forward flight case, except the Q matrix associated with the weight and balance states equals 2000.

During the pure hover portion of the maneuver, the parameters with better estimation performance (gross weight, station line, and butt line) perform reasonably well in adjusting to a new weight and balance condition. The less observable parameter (water line) does a poor job. After slight maneuvering occurs at $t = 5$ s, the parameter estimates immediately begin correcting themselves as soon as some angular rates are present. Just like the forward flight case, the water line estimate moves fastest when a roll rate is present.

To explore the performance of the weight and balance estimation algorithm under nonideal conditions, the algorithm was exercised with a Monte Carlo simulation with sensor and model error. A total of 250 sample runs were performed for both sensor error and model error. The maneuver used for the Monte Carlo simulations is the

Table 1 Results from Monte Carlo simulations with measurement error

Parameter	Mean	Standard deviation	Correct value
Gross weight	2554.9 lbf	19.39 lbf	2550.0 lbf
c.g. station line	100.005 in.	0.0816 in.	100.0 in.
c.g. butt line	0.009 in.	0.1086 in.	0.0 in.
c.g. water line	49.54 in.	1.23 in.	49.6 in.

Table 2 Results from Monte Carlo simulations with model error

Parameter	Mean	Standard deviation	Correct value
Gross weight	2551.7 lbf	30.15 lbf	2550.0 lbf
c.g. station line	99.99 in.	0.0476 in.	100.0 in.
c.g. butt line	-0.009 in.	0.0573 in.	0.0 in.
c.g. water line	49.39 in.	1.81 in.	49.6 in.

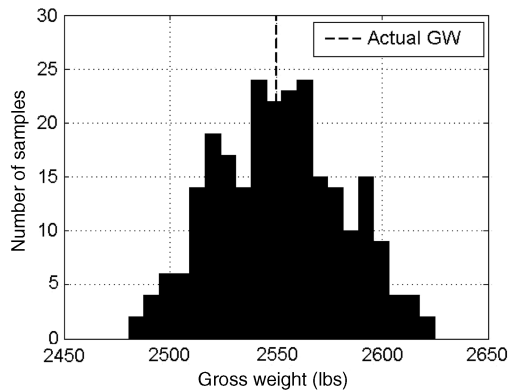


Fig. 21 Histogram of gross weight estimation with model error; (GW denotes gross weight).

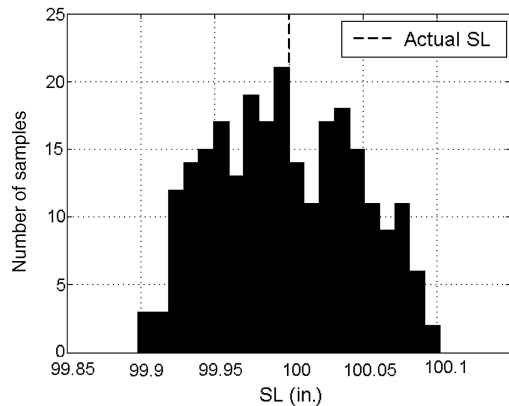


Fig. 22 Histogram of mass center station line estimation with model error; (SL denotes station line).

same forward flight maneuver that is outlined in Figs. 4–7. Sensor errors were included in the Monte Carlo simulation by adding bias and noise to each sensor output. The standard deviation for bias and noise was 3.3 ft for position states, 0.2 deg for attitude states, 1.0 ft/s for velocity states, and 0.6 deg/s for angular rates. The Figs. 17–20 show histograms of the Monte Carlo results for the sensor error case. The results are also summarized in Table 1. The mean estimation values and associated standard deviations for gross weight, mass center station line, and mass center butt line are accurate and tightly bound, while the water line estimation is fairly poor and exhibits a standard deviation which is a notable percentage of the practical range of the water line (mean = 49.53 in., std = 1.23 in.). Model error was included in the Monte Carlo simulation by creating a model mismatch between the actual helicopter model and the internal helicopter model employed by the estimator. The vehicle geometry, baseline moments of inertia, and aerodynamic data were all altered slightly in each of the 250 simulations. Some example values of model error are 0.3 lbs for main rotor blade weight, 0.02 ft for main rotor radius, and 2% for normalized aerodynamic coefficients. The algorithm showed a similar level of robustness to model error with accurate mean estimation values and standard deviations. The results are summarized in Table 2. Figures 21–24 present histograms of Monte Carlo simulation results for the model error case. While the results for all the parameters in the model error case show the same trends as the sensor error case, the standard deviation in estimations tend to be slightly larger due to the fact that the model error induces more severe estimation errors than sensor errors.

The biggest hurdle for practical implementation of this method is minimizing the influence of modeling errors. It is expected that the best way for this problem to be addressed is to make use of a model that adaptively estimates and subsequently cancels model mismatch. Adaptive methods have become increasingly used in air vehicle flight control and would serve to enhance the algorithm presented

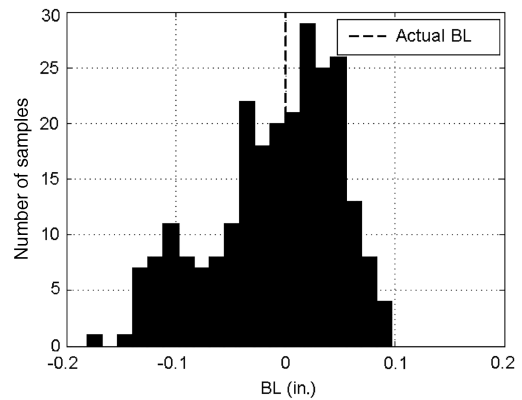


Fig. 23 Histogram of mass center butt line estimation with model error; (BL denotes butt line).

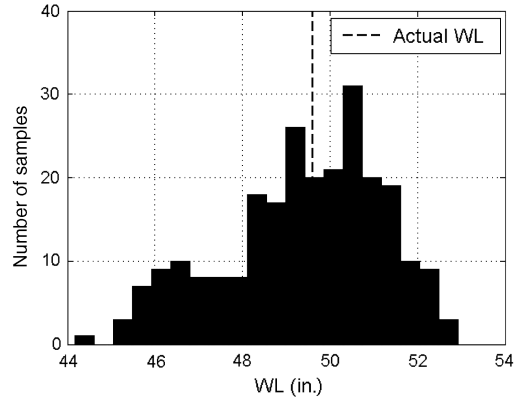


Fig. 24 Histogram of mass center water line estimation with model error; (WL denotes water line).

here. Testing such a system is beyond the scope of this paper and is left to further work. The results presented here demonstrate the capability of the extended Kalman filter to accurately estimate weight and balance parameters in rotorcraft when paired with a flight dynamic model of acceptable fidelity.

V. Conclusions

By casting estimation of weight and mass center location as a state estimation problem, the machinery of extended Kalman filtering can be employed for in-flight and real-time estimation of rotorcraft weight and balance. The presented algorithm is shown to work well in both hover and forward flight, provided sufficient motion is present to render the parameters observable. Also, the method works well in cases where loads are dropped or picked up in flight. Typically the algorithm quickly estimates station line and butt line mass center position and more slowly converges on helicopter weight and water line. The algorithm is also shown to be reasonably robust to sensor and model errors. While further work is necessary to investigate the details of implementation challenges, the extended Kalman filter provides a successful framework for estimating weight and balance parameters and is reasonably robust to measurement and modeling errors. By combining the extended Kalman filter with traditional flight dynamic models to estimate gross weight and mass center location, this work has introduced a novel solution to a pressing problem.

References

- [1] Moffatt, J., "Helicopter Gross Weight Determination from Monitored Parameters," U.S. Army Aviation and Troop Command, Fort Eustis, VA, Final Technical Report, ADA311339, 1986.
- [2] Morales, M., and Haas, D., "Feasibility of Aircraft Gross Weight Estimation Using Artificial Neural Networks," *Proceedings of the 57th American Helicopter Society International Annual Forum*, American

- Helicopter Society, 2001, pp. 1872–1880.
- [3] Idan, M., Iosilevskii, G., and Nazarov, S., “In-Flight Weight and Balance Identification Using Neural Networks,” *Journal of Aircraft*, Vol. 41, No. 1, 2004, pp. 137–143.
doi:10.2514/1.592
- [4] Teal, R., Evernham, J., Larchuk, T., Miller, D., Marquith, D., White, F., and Diebler, D., “Regime Recognition for MH-47E Structural Usage Monitoring,” *Proceedings of the 53rd Annual Forum*, American Helicopter Society, 1267–1284.
- [5] Talbot, P. D., Tinning, B. E., Decker, W. A., and Chen, R. T. N., “A Mathematical Model of a Single Main Rotor Helicopter for Piloted Simulation,” NASA TM-84281, Sept. 1982.
- [6] Duval, R., “A Real-Time Multi-Body Dynamics Architecture for Rotorcraft Simulation, the Challenge of Realistic Rotorcraft Simulation,” *RaeS Conference*, Royal Aeronautical Society, Paper 0129, Nov. 2001.
- [7] Lewis, M., and Aiken, E., “Piloted Simulation of One-on-One Helicopter Air Combat at NOE Flight Levels,” NASA TM-86686, U.S. Army Aviation Systems Command, Ames Research Center, Moffett Field, CA, 1985.
- [8] Prouty, R. W., “Stability and Control Analysis,” *Helicopter Performance, Stability and Control*, Krieger, Malabar, FL, 1986, pp. 559–560.
- [9] Stengel, R., *Optimal Control and Estimation*, Dover, New York, ISBN 0-486-68200-5, 1994, pp. 340–361.
- [10] Kanjilal, P., *Adaptive Prediction and Predictive Control*, Institution of Electrical Engineers Control Engineering Series, Peter Peregrinus Ltd, London, United Kingdom, ISBN 0 86341 193 2, 1995.
- [11] Siegel, E., “Stability and Control Data Summary for Single Rotor Helicopter, Hughes OH-6A,” Hughes Helicopter Report 369-V-8010, April 28, 1975.